Kinetic Investigations on the UV-Induced Photopolymerization of Nanocomposites by FTIR Spectroscopy

Fusheng Li, Shuxue Zhou, Bo You, Limin Wu

Department of Materials Science and The Advanced Coatings Research Center of China Educational Ministry, Fudan University, Shanghai 200433, People's Republic of China

Received 22 July 2003; accepted 18 April 2005
DOI 10.1002/app.22629
Published online in Wiley InterScience (www.interscience.wiley.com).

ABSTRACT: The kinetics of the photopolymerization for nanocomposites containing nanosilica with 2,2-dimethoxy-1,2-diphenylethan-1-one or benzophenone/*n*-methyl diethanolamine (BP/MDEA)as photoinitiators were studied by FTIR spectroscopy. It was found that nanocomposites containing nanosilica had higher conversion in comparison with pristine EA. The presence of MPS and ethanol accelerated the photopolymerization of nanocomposites, while the presence of water decelerated it. The photopolymerization of nanocomposites was more sensitive to oxygen than that of pristine EA. © 2005 Wiley Periodicals, Inc. J Appl Polym Sci 99: 1429–1436, 2006

Key words: nanosilica; nanocomposite coatings; photopolymerization kinetics; UV curing

INTRODUCTION

Nanocomposites are a new kind of composite materials[1–5] with an ultrafine phase dispersed in 1–100 nm size, and show very interesting properties markedly different from the conventional ones. As a subdivision part of nanocomposites, UV-curable nanocomposites combine the advantages of UV curing process and nanotechnology together and therefore impart the materials some unique properties,[6,7] finally getting a wide-range usage in the fields such as coatings, printings, inks, adhesives and so on.[8,9]

Although there are many papers focusing on the kinetics of conventional UV-curable coatings,[10,11] few have ever been concerned with the kinetics of UV-curable nanocomposites coatings. The reported research work mainly concentrates on the synthesis and characterization of the resultant UV-curable nanocomposites films.[12–15] However, the kinetics study is also very important to understand the final property and microstructure of UV-curable nanocomposites because the advantages of UV-curing are shown on its curing process rather than on the resultant materials properties.

There are several methods such as FTIR,[16] DSC,[17] NMR,[18] Raman spectroscopy,[19] near-infrared reflection spectroscopy,[20] dilatometric monitoring of volume contraction,[21] holographic technique,[22] electrical resistance, and rheological methods[23] to investigate the kinetics of photopolymerization. Recently, Falk et al.[23] tried to use optical pyrometry to characterize the photopolymerization kinetics. Among all the methods, differential scanning calorimetry(DSC) is by far the most widely used technique in photocuring kinetic studies. But this method has several drawbacks, one of them is its relatively long response time (~2 s), which makes it impossible to monitor polymerization reactions accurately.

FTIR method has been used as an important method for characterizing the photopolymerization kinetics of UV-curable coatings even from the inception of the discovery and development of photoinduced polymerizations. In this paper, we tried to use FTIR method to investigate the kinetics of photopolymerization of nanocomposites induced by the UV irradiation of wavelength 365 nm and 2,2-dimethoxy-1,2-diphenylethan-1-one (Irgacure 651) or benzophenone/*n*-methyl diethanolamine(BP/MDEA) as photoinitiators. The article seeks to understand photopolymerization mechanism in nanosilica-embedded nanocomposites. The influences of photoinitiator type and content, nanosilica content, light intensity, oxygen inhibition, and impurities (such as ethanol, water, MPS) on polymerization rate and double bond conversion were investigated as well.

EXPERIMENTAL

Materials

Tetraethyl orthosilicate (TEOS) and 3-(trimethoxysilyl) propyl methacrylate (MPS) were both purchased

Correspondence to: L. Wu (lxw@fudan.ac.cn).

from Shanghai Huarun Chemical Company of China. *n*-Butyl acetate, absolute ethanol(EtOH) and ammonia solution (25–28% ammonia content) were purchased from Shanghai Chemistry Reagent Co. Ltd. *n*-Methyl diethanolamine(MDEA) and benzophenone(BP) were provided by Changzhou Wujin No. 5 Chemical Factory. 2,2-Dimethoxy-1,2-diphenylethan-1-one (Irgacure 651) is a gift of Ciba Specialty Chemicals. Trimethylolpropane triacrylate (TMPTA) and epoxy acrylate(SM6104, M_w = 1000, viscosity = 30,000 mPa s at 60°C) were the products of Changxing Corp. and Sanmu Corp. of China, respectively. All these materials were used as received, without further purification.

Preparation and modification of colloidal silica particles

Colloidal silica particles with an average size of 40 nm were prepared by sol-gel method.[12] The molar ratio of $EtOH/NH_3/H_2O/TEOS$ was 9 : 0.2 : 2.5 : 1. TEOS and fractional absolute alcohol was first charged in three-necked round bottom flask, then the residual absolute alcohol, deionized water and ammonia were dropped within 0.5 h. The mixture was kept at 50°C and stirred overnight. After that, MPS was added based on the weight ratio of 3 : 14 for MPS/TEOS and the reaction continued for another 6 h. The resulted nanosilica sol was condensed under vacuum at 50°C to remove almost all the water and ethanol to obtain MPS-modified nanosilica particles for further use.

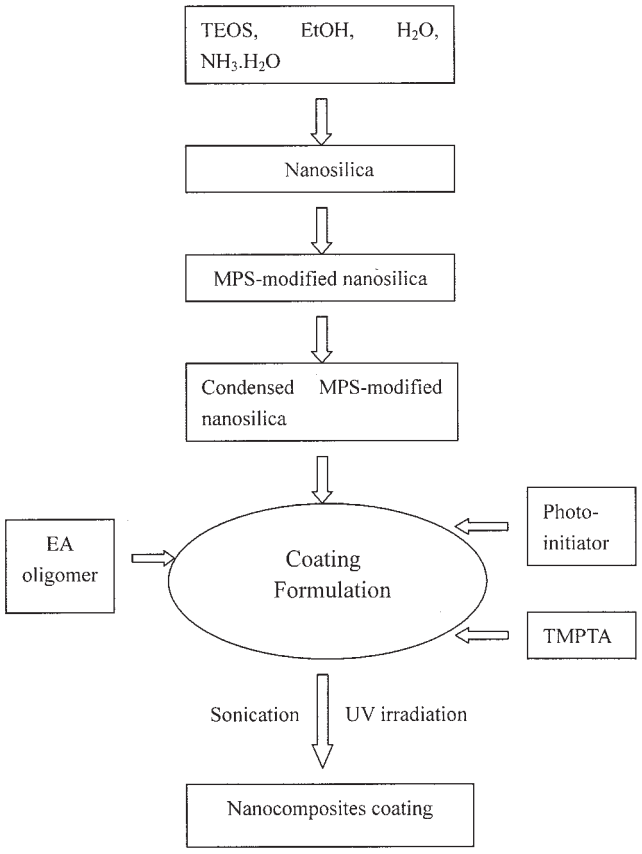

Figure 1 Schematic diagram of the process for preparing nanocomposites coatings.

TABLE I
Formulation for Preparation of EA/SiO_2 Nanocomposite Coats

Sample code	Epoxy acrylate (%)	SiO_2 mixture (%)	TMPTA (%)	Irgacure 651 (%)	BP/MDEA (%)
A		0	57	3	
B		0	57		1.8/1.2
C		20	39	1	
D		20	37	3	
E	40	20	35	5	
F		20	37		1.8/1.2
G		5	52	3	
H		10	57	3	
I		30	27	3	

Preparation of nanocomposites

The condensed nanosilica was added into TMPTA and treated with ultrasonication for 30 min and then added into EA oligomeric resin and ultrasonicated for another 30 min, followed by addition of photoinitiators. The schematic diagram for the preparation is shown in Figure 1. The formulations are summarized in Table I. The nanocomposites coatings were irradiated by an ultraviolet curing apparatus (UV Crosslinker, Spectroline company, US), with a wavelength of 365 nm.

UV curing kinetics of nanocomposites

The FTIR spectra of samples before curing and after different UV curing time were scanned by a Magna-IR™ 550 spectrometer (Nicolet Instruments, Madison, WI). In this study, the sandwich-like NaCl plates was used for the FTIR scanning to minimize the influence of atmospheric oxygen. Unless otherwise noted, all the samples were investigated in the laminate state (sandwich-like) and the thickness of nanocomposites is about 20 μm.

RESULTS AND DISCUSSION

Preparation of MPS-modified nanosilica particles from sol–gel method

The size of the nanosilica particles prepared in our lab was 40 nm based on TEM observation using 9 : 0.2 : 2.5 : 1 (mol ratio) of $EtOH/NH_3/H_2O/TEOS$. Since nanosilica particles prepared by sol-gel method are usually hydrophilic and tend to aggregate in the organic dilutes

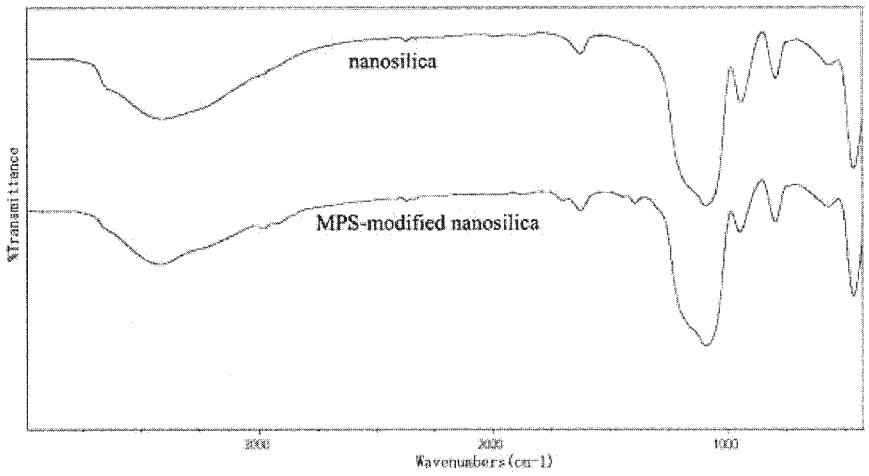

Figure 2 FTIR spectra of unmodified nanosilica and MPS-modified nanosilica particles.

or polymers, they have been modified with MPS in this study. The FTIR spectrum of MPS-modified nanosilica powders (after purification) and nanosilica without modification are shown in Figure 2. Relative to the spectrum of unmodified nanosilica particles, a new absorbing peak at 1725 cm^{-1} assigned to C = O stretching vibration is observed in the spectrum of MPS-modified nanosilica particles, indicating MPS has been successfully attached to the surfaces of nanosilica particles.

Typical photopolymerization kinetics of nanocomposites and the calculations involved

The typical FTIR spectra of UV-curable nanocomposite coatings with different irradiation times are illustrated in Figure 3. It is found that the intensity of the peak at 1635 cm^{-1} for C = C stretching absorbance decreases with increasing time of exposure to UV irradiation. Since the peak at 1635 cm^{-1} is well separated from other peaks, it is usually used to quantify the conversion of C = C bond in UV-curable coatings. Another peak at 1725 cm^{-1} due to C = O stretching absorbance is designated as the reference peak for its invariability[24] during UV curing. Thus, the percentage of conversion (C) of C = C bond can be calculated according to the following equation:

$$C = 100 \times (1 - A_t S_0 / A_0 S_t) \quad (1)$$

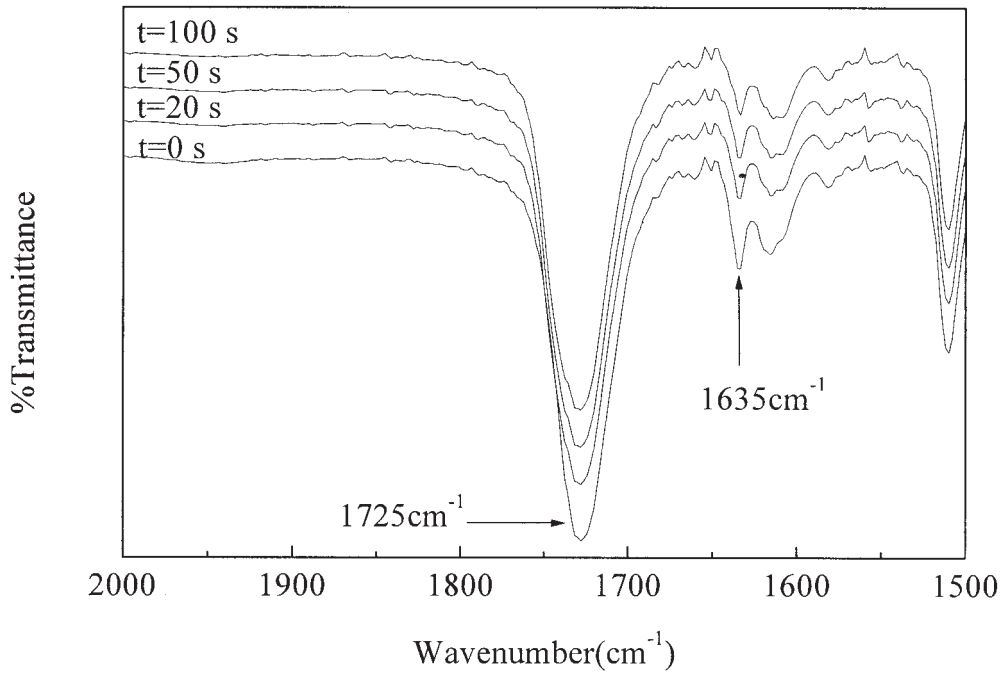

Figure 3 The FTIR spectra of UV nanocomposite coatings at different irradiation times (2.8 mW/cm^2, 3 wt % Irgacure 651).

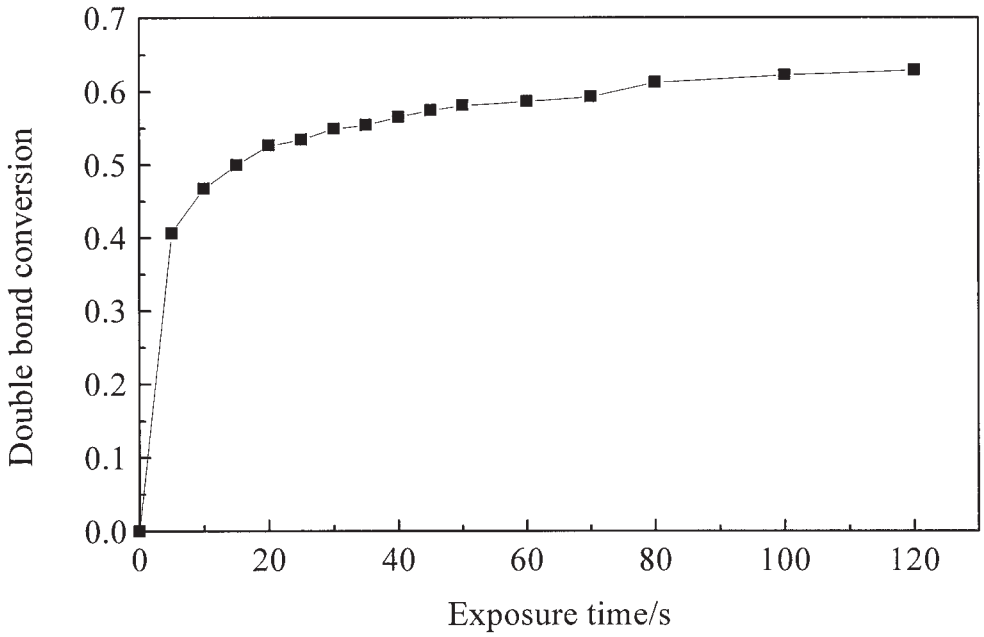

Figure 4 The plot of photopolymerization kinetics of nanocomposites (3 wt % Irgacure 651, 2.8 mW/cm^2 at 365 nm).

where A_t and A_0 are the areas of the 1635 cm^{-1} peak and S_t, S_0 the areas of 1725 cm^{-1} peak at time t, and $t = 0$, respectively.

Based on the data calculated by eq. (1), the conversion curves for the UV-curable nanocomposite coatings containing 20 wt % nanosilica content are plotted in Figure 4. Its induction time at the beginning of photopolymerization is negligible. Then an acceleration of the polymerization rate is observed because of gel effect. After that, the polymerization rate slowed down because of the vitrification of the resin. This is consistent with the typical kinetic curve of the UV-curable coatings with three functionally reactive dilutes.[6]

Effect of the photoinitiator type and content

The photopolymerization kinetic curves for pristine EA and the nanocomposites coatings with Irgacure 651 or BP/MDEA as initiators were plotted in Figure 5. It can be seen that the final conversions of C = C bonds for nanocomposites are higher than those of pristine EA whether initiated by Irgacure 651 or BP/MDEA. However, under the same photoinitiator concentration, the UV coating with BP/MDEA as the photoinitiator has a slower photopolymerization rate and a longer induction time than that initiated by Irgacure 651. This phenomenon can be easily explained based on their distinctive initiating mechanism: the Irgacure 651 is Norrish type I photoinitiator, which undergoes a direct photofragmentation process (α- or less common β-cleavage)[25] (Fig. 6). Under the UV radiation, 2 mol primary radicals can be obtained from 1 mol Irgacure 651 (Fig. 6). Those 2 mol primary radicals can react with the monomers and dissolve oxygen. So the oxygen dissolved in the formulation can be consumed instantly. As for the BP/MDEA initiating system, it is not so efficient as Irgacure 651, because it belongs to the Norrish type II photoinitiator involving a primary process of hydrogen atom abstraction from the MDEA (tertiary amine),[25] only 1 mol primary radicals can react with the monomer though there are 2 mol primary radicals formed (Fig. 6). As a result, long induction time was observed for the BP/MDEA system.

The effect of the photoinitiator concentration on the polymerization rate of nanocomposites irradiated by

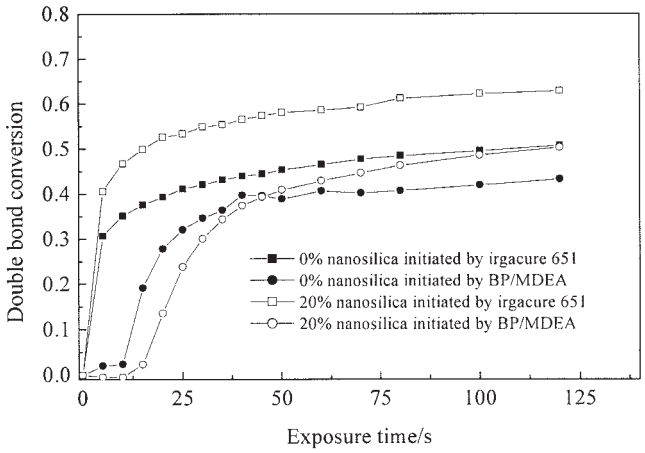

Figure 5 Influence of photoinitiator type on photopolymerization kinetics (3 wt % initiators, 2.8 mW/cm^2 at 365 nm).

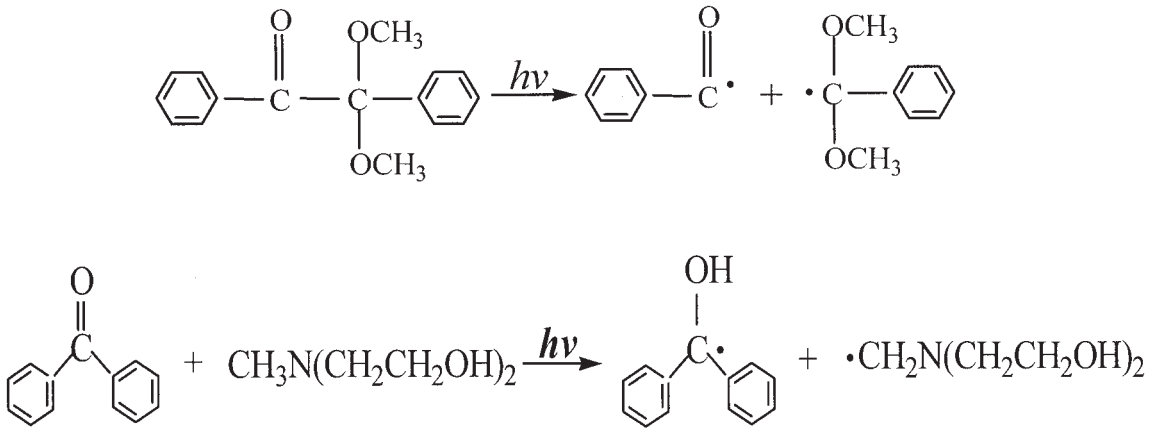

Figure 6 Photolysis of Irgacure 651 and BP/MDEA.

UV ray is presented in Figure 7. An increase of the initiator content strongly accelerates the photopolymeriztion of the nanocomposites. However, the residual photoinitiator will affect the property of resultant nanocomposites at high photoinitiator concentration. So in our study 3% Irgacure 651 was chosen for kinetics study.

Effect of the nanosilica content

Figure 8 shows the effect of nanosilica content on the double bond conversion of nanocomposites with curing time. It can be seen that as the nanosilica content increases, the curing rate accelerates and reaches the highest at ~10 wt % loading. However, above this critical point, an observable decrease of curing speed is observed with the increasing nanosilica loading. The reason for this phenomenon is unclear. But a similar phenomenon was also observed in the UV coating containing organically modified layered silicate, reported by Uhl et al.[13] The increment in curing speed at lower nanosilica content suggests that the presence of nanosilica enhances the curing reaction, may be resulting from inhibition effect of the inorganic network on bimolecular termination.[26,27]

Effect of impurities

Introducing the nanosilica sol into the polymer system will inevitably bring some impurities (such as ethanol, water, MPS) into the resin system.[28] However, there are very few papers available dealing with influence

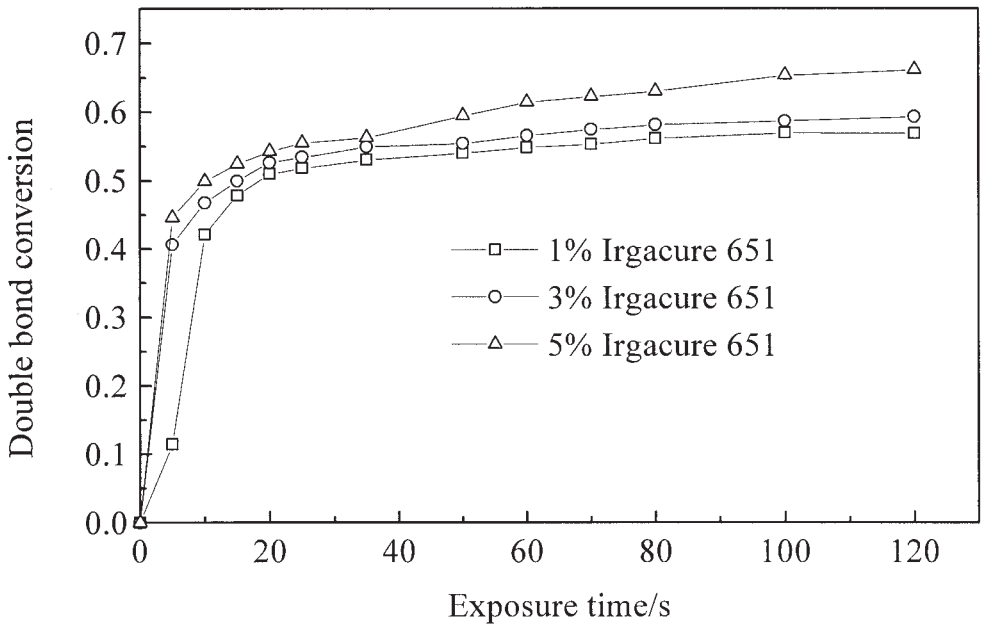

Figure 7 Influence of photoinitiator content on photopolymerization kinetics (20 wt % nanosilica, 2.8 mW/cm^2 at 365 nm).

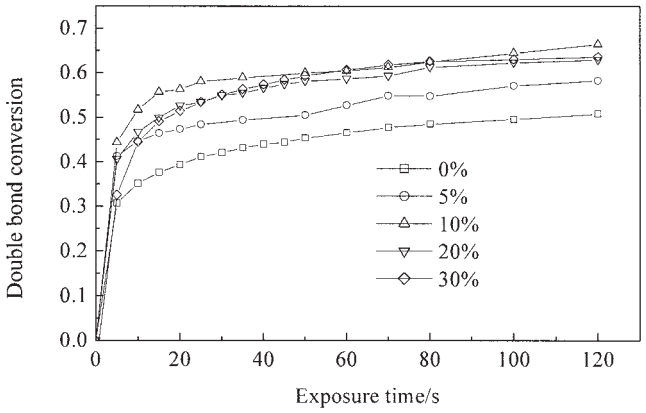

Figure 8 Influence of nanosilica content on photopolymerization kinetics (3 wt % Irgacure 651, 2.8 mW/cm^2 at 365 nm).

of those impurities on the photopolymerization kinetics. To understand the photopolymerization mechanism of nanocomposites further, the effects of ethanol, water, and MPS on the photopolymerization kinetics of nanocomposites are investigated as well in this study, as illustrated in Figure 9. It can be seen that the photopolymeriztion speed is accelerated and final conversion enhances when the UV nanocomposite coatings contain ethanol or MPS. After radiation for 90 s, the double bond conversion can reach 73 and 70% for the nanocomposites containing ethanol and MPS, respectively, while only 62% for the nanocomposites without impurities. The increment of curing speed and final double bond conversion of nanocomposites containing ethanol may be due to the plasticizing effect of ethanol which can enhance the mobility of monomer and polymer radical chain, while those containing MPS may be attributed to the more silica inorganic structure formed, which will trap more oxygen in the photopolymerization system because of

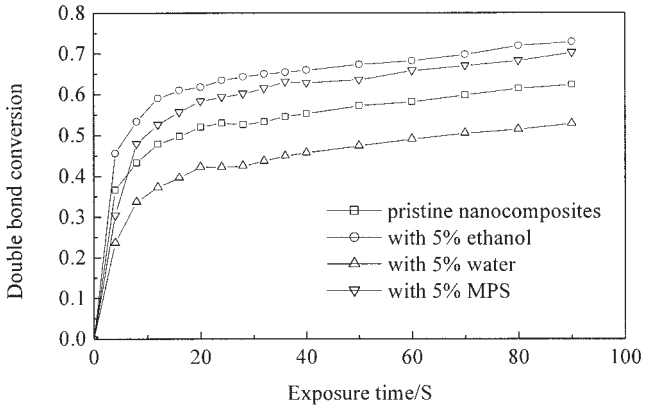

Figure 9 Influences of ethanol, water, and MPS on photopolymerization kinetics (3 wt % Irgacure 651, 2.8 mW/cm^2 at 365 nm).

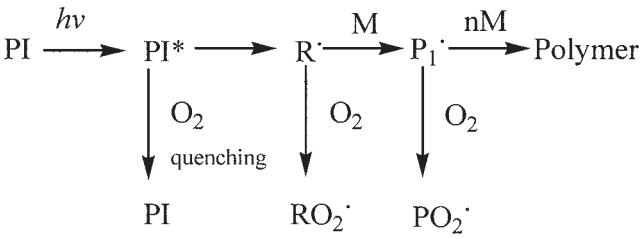

Figure 10 Oxygen inhibition in a radical-type photoinitiated polymerization.

high affinity of Si for O_2.[26] Contrary to ethanol and MPS, water decreases the photopolymeriztion speed and final double bond conversion. After radiation for 90 s, the double bond conversion only reaches 53% for the nanocomposites containing water. This may have resulted from the bad compatibility of water with Irgacure 651.

Effect of oxygen

The triplet states of photoinitiators and radicals formed from photoinitiators are strongly attacked by oxygen leading to quenching and the formation of peroxy radicals, respectively. The detrimental effect of oxygen on radical photopolymerization reactions is well known from curing process performed with photoinitiators. So there are many reports dealing with the oxygen inhibition effect on the radical photopolymerization in the presence of air.[29,30]

Specifically, the oxygen inhibition effect was realized mainly by the quenching the triplet state photoinitiator, primary radicals, polymer radicals,[29] as indicated in Figure 10.

A simple means to investigate the influence of molecular oxygen on photopolymerization of nanocomposites is to compare the kinetics in aerated and laminated systems. Figure 11 presents the photopolymer-

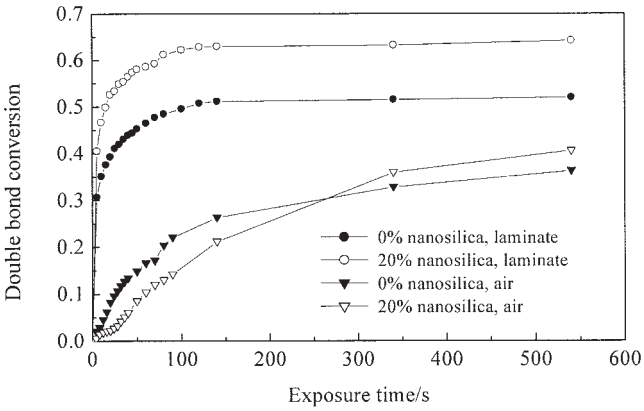

Figure 11 Photopolymerization kinetics in air state and laminate state (3 wt % Irgacure 651, 2.8 mW/cm^2 at 365 nm).

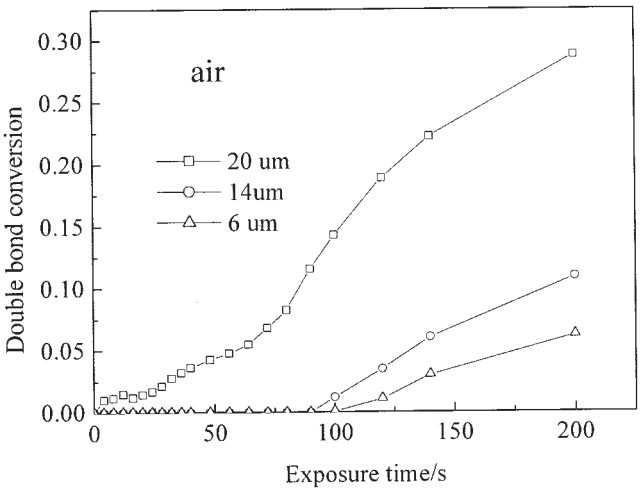

Figure 12 Effect of film thickness on photopolymerization kinetics in the presence of oxygen (3 wt % Irgacure 651, 2.8 mW/cm^2 at 365 nm).

ization kinetics of pristine EA and nanocomposites containing 20 wt % nanosilica in air and the laminate state. From Figure 11, it can be seen that the nanocomposites has a lower curing rate in air in comparison with the UV-curable coating in the laminate state, indicating inhibition effect of atmospheric air on nanocomposites photopolymerization is relatively stronger.[30] However, with the prolongation of exposure time, the surface of film reaches a certain double bond conversion and the permeability of oxygen to the bulk of film is therefore reduced greatly. As a result, the effect of oxygen on the whole photopolymerization of nanocomposites diminishes to the lowest level and therefore the inhibition effect of inorganic network on bimolecular termination dominates the whole photopolymerization process which can accelerate the curing rate greatly.[26,27] So after a certain time, *e.g.*, 300 s in this study, the final double bond conversion of nanocomposistes becomes higher than that of pristine EA cured in air.

Effect of film thickness

Another critical factor influencing the inhibitory effect of oxygen is film thickness. Figure 12 demonstrates the influence of film thickness on the photopolymerization kinetics. From which it can be seen the double bond conversion of nanocomposites decreases with decreasing film thickness. This result is consistent with photopolymerization behavior of all organic films in the presence of oxygen, because the oxygen diffusion process dominates in this case.[31]

Effect of light intensity

It is reported that the oxygen content in silicone-acrylate is four times as high as that in other monomers because of its high permeability.[30] So compared with pristine EA system, the nanocomposite system was affected by the oxygen more obviously and thus more sensitive to the irradiation intensity, considering that higher light intensity can conquer the oxygen inhibition more effectively.[32]

Figure 13 shows the plots of photopolymerization for pristine acrylate system and nanocomposites under different irradiation intensity. It can be seen that the photopolymerization rate and final double bond conversion increase as light intensity increases for both pristine EA and UV nanocomposite coatings. However, the increment is more obvious for UV nanocomposite coatings than for pristine EA. This may be attributed to decreasing oxygen effect with increasing irradiation intensity, especially on the nanocomposites.

CONCLUSIONS

FTIR spectroscopy was used to study the photopolymerization kinetics of nanocomposites based on the epoxy acrylate and nanosilica with Irgacure 651 or BP/MDEA as photoinitiators. It is found that nanocomposites containing nanosilica has increasing photopolymerization rate independent of photoinitiator type. The presence of ethanol or MPS accelerates the photopolymerization of nanocomposites, while the presence of water decreases the curing speed. Compared with pristine EA, nanocomposite is more sensitive to oxygen. In addition, the photopolymerization behaviors of nanocomposites at different UV radiation intensity, various film thickness, and different photoinitiator concentration are similar to those of the pristine EA cured under the same condition.

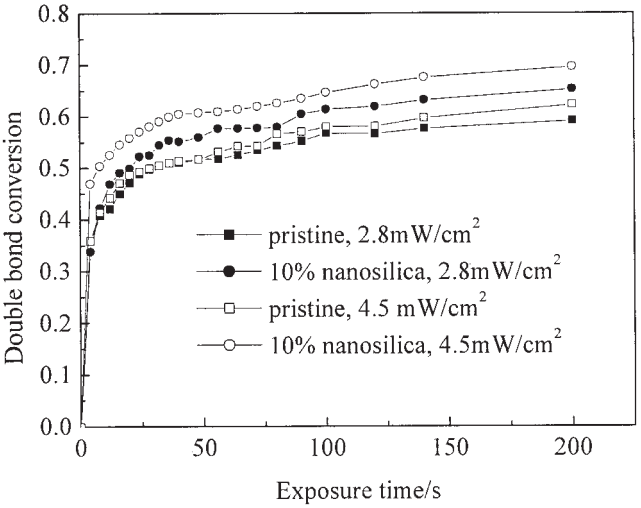

Figure 13 Effect of UV radiation intensity on photopolymerization kinetics (3 wt % Irgacure 651, at 365 nm).

The authors thank National "863" Foundation, Shanghai Special Nano Foundation, Shanghai Economic commission Industrialization Foundation, the Doctoral Foundation of University, Trans-century Outstanding Talented Person Foundation of China Educational Ministry, Key Project of China Educational Ministry for the financial support for this research.

References

1. Benfarhi, S.; Decker, C.; Keller, L.; Zahouily, K. Eur Polym Mater 2004, 40, 493.
2. Bauer, F.; Glasel, H.; Decker, U.; Ernst, H.; Freyer, A.; Hartmann, E.; Sauerland, V.; Mehnert, R. Prog Org Coat 2003, 47, 147.
3. Becker, O.; Varley, R. J.; Simon, G. P. Eur Polym Mater 2004, 40, 187.
4. Torre, L.; Frulloni, E.; Kenny, J. M.; Manferti, C.; Camino, G. J Appl Polym Sci 2003, 90, 2532.
5. Dong, W.; Zhu, C. Mater Lett 2000, 45, 336.
6. Bajpai, M.; Shukla, V. Pigm Resin Technol 2003, 32, 382.
7. Stowe, R. W. Met Finishing 2002, 8, 8.
8. Wenning, A. Macromol Symp 2002, 187, 597.
9. Hwang, D. K.; Moon, J. H.; Shul, Y. G.; Jung, K. T.; Kim, D. H.; Lee, D. W. J Sol-Gel Sci Technol 2003, 26, 783.
10. Decker, C. Polym Int 1998, 45, 133.
11. Decker, C. Pigm Resin Technol 2001, 30, 278.
12. Suratwala, T. I.; Hanna, M. L.; Miller, E. L.; Whitman, P. K.; Thomas, I. M.; Ehrmann, P. R.; Maxwell, R. S. J Non-Cryst Solids 2003, 316, 349.
13. Uhl, F. M.; Davuluri, S. P.; Wong, S. C.; Webster, D. C. Chem Mater 2004, 16, 1135.
14. Decker, C.; Zahouily, K.; Keller, L.; Benfarhi, S.; Bendaikha, T.; Baron, J. J Mater Sci 2002, 37, 4831.
15. Muh, E.; Stieger, M.; Klee, J. E.; Frey, H.; Mulhaupt, R. J Polym Sci Part A: Polym Chem 2001, 39, 4274.
16. Scherzer, T.; Decker, U. Radiat Phys Chem 1999, 55, 615.
17. Maffezzoli, A.; Terzi, R. Thermochim Acta 1998, 321, 111.
18. Katoh, E.; Sugisawa, H.; Oshima, A.; Tabata, Y.; Seguchi, T.; Yamazaki, T. Radiat Phys Chem 1999, 54, 165.
19. Pamell, S.; Min, K.; Cakmak, M. Polymer 2003, 44, 5137.
20. Scherzer, T.; Mehnert, R.; Lucht, H. Macromol Symp 2004, 205, 151.
21. Anseth, K. S.; Bowman, C. N.; Peppas, N. A. J Polym Sci Part A: Polym Chem 1994, 32, 139.
22. Carre, C.; Lougnot, D. J; Fouassier, J. P. Macromolecules 1989, 22, 791.
23. Falk, B.; Vallinas, S. M.; Crivello, J. V. J Polym Sci Part A: Polym Chem 2003, 41, 579.
24. Wang, J. Z. Y.; Bogner, R. H. Int J Pharm 1995, 113, 113.
25. Allen, N. S. J Photochem Photobiol A Chem 1996, 100, 101.
26. Soppera, O.; Barghorn C. C. J Polym Sci Part A: Polym Chem 2003, 41, 716.
27. Soppera, O.; Barghorn C. C. J Polym Sci Part A: Polym Chem 2003, 41, 831.
28. Crivello, J. V.; Mao, Z. B. Chem Mater 1997, 9, 1562.
29. Studer, K.; Decker, C.; Beck, E.; Schwalm, R. Prog Org Coat 2003, 48, 101.
30. Studer, K.; Decker, C.; Beck, E.; Schwalm, R. Prog Org Coat 2003, 48, 92.
31. Guizard, C.; Bac, A.; Barboiu, M.; Hovnanian, N. Sep Purif Technol 2001, 25, 167.
32. Awokola, M.; Lenhard, W.; Loffler, H.; Flosbach, C.; Frese, P. Prog Org Coat 2002, 44, 211.